Plastic sliding of charge density waves: X-ray space resolved-studies versus theory of current conversion

S. Brazovskii
Laboratoire de Physique Théorique et des Modèles Statistiques, Centre National de la Recherche, Bât.100, Université Paris-Sud, 91405 Orsay, Cedex, France
and Landau Institute, 2, Kosygina St., GSP-1, 117940 Moscow, Russia

N. Kirova
Laboratoire de Physique Théorique et des Modèles Satistiques, Centre National de la Recherche, Bât.100, Université Paris-Sud, 91405 Orsay, Cedex, France

H. Requardt*
Centre de Recherches sur les Très Basses Températures, laboratoire associé à l'Université Joseph Fourier, Centre National de la Recherche Scientifique, Boîte Postale 166, 38042 Grenoble, Cedex 9, France
and Institut Laue Langevin, Boîte Postale 156, 38042 Grenoble, France

F. Ya. Nad
Centre de Recherches sur les Très Basses Températures, laboratoire associé à l'Université Joseph Fourier, Centre National de la Recherche Scientifique, Boîte Postale 166, 38042 Grenoble, Cedex 9, France
and Institute of Radio-Engineering and Electronics, 103907 Moscow, Russia

P. Monceau
Centre de Recherches sur les Très Basses Températures, laboratoire associé à l'Université Joseph Fourier, Centre National de la Recherche Scientifique, Boîte Postale 166, 38042 Grenoble, Cedex 9, France

R. Currat
Institut Laue Langevin, Boîte Postale 156, 38042 Grenoble, France

J. E. Lorenzo
Laboratoire de Cristallographie, Centre National de la Recherche Scientifique, Boîte Postale 166, 38042 Grenoble, France

G. Grübel and Ch. Vettier
European Synchrotron Radiation Facility, Boîte Postale 220, 38043 Grenoble, France
(Received 7 September 1999)

We present experimental and theoretical results on the distribution of deformations experienced by a sliding charge density wave (CDW) in connection with the normal $\rightleftharpoons$collective current conversion process. High-resolution (30–100 μm) x-ray measurements of the satellite positional shift q have been performed on $NbSe_3$ whiskers at 90 K. For the first time q has been determined with application of direct, as well as pulsed, currents and in the immediate vicinity of the injection extraction contact. We observe a steep variation of q near the contact that we model in terms of intensive nucleation processes of dislocation loops (DLs) at the host defects. A logarithmic time decay between pulses implies a creep of pinned DLs. A small constant residual gradient in the central part of the sample indicates that the conversion process is incomplete, consistent with a finite DL pinning threshold. On the theory side, general equations are derived to describe inhomogeneous distributions of deformations, electric fields, and currents. Numerical modeling under realistic experimental conditions is combined with model-independent relations. We discuss both similarities and contradictions with earlier studies.

I. INTRODUCTION

Phase slippage is a common phenomenon[1] in condensed matter systems with complex order parameters. Phase gradients in the condensate, as originating, e.g., from external forces, cannot grow indefinitely. Beyond some critical value, the strain associated with the phase gradient is released through 2π phase jumps. The process is repetitive in time, with a rate dependent on the magnitude of the external force. Phase slippage has been intensively studied in narrow superconducting channels,[2,3] in superfluid helium,[4] and in quasi-one-dimensional (1D) CDW systems. In the latter case, below the Peierls transition temperature T_P, the system is characterized by a modulated electronic density $\rho(x) = \rho_0[1+\alpha\cos(Q_0x+\varphi)]$ together with a periodic lattice distortion of the same wave number $Q_0=2k_F$ where k_F is the

(generally incommensurate) Fermi momentum. The new periodicity opens a gap in the electron density of states and leads to new (satellite) Bragg peaks. CDW pinning by host defects fixes the local phase φ and destroys the translational invariance of the CDW ground state. Application of an electric field $\mathcal{E}$ above a threshold value $\mathcal{E}_t$, sets the CDW in motion and gives rise to a collective current.[5–8]

Phase slippage is required at the electrodes for the conversion from free to condensed carriers.[9–11] When the CDW is depinned between current contacts, CDW wave fronts are created near one electrode and destroyed near the other, leading to CDW compression at one end and stretching at the other end. In a purely 1D channel, the order parameter is driven to zero at a certain distance from the pinning ends.[9] For samples of finite cross section, phase slippage develops as dislocation loops (DLs) (see Refs. 12 and 13), which climb to the crystal surface, each DL allowing the CDW to progress by one wavelength.[10] In quasi-one-dimensional systems the phase slips are nucleated already at the microscopic level of a single chain. It has been shown[14,15] that a free electron is not stable against a fast ($\omega_{\rm ph}^{-1}$) conversion into an amplitude soliton (here the amplitude passes through zero which is a general necessary condition for the phase slips to occur). This dynamic stage is not yet sufficient since only a pair of electrons can complete the 2π phase slip. It happens in the course of a relatively slow kinetic stage when pairs of amplitude solitons aggregate into the 2π ones.

Effects of the current conversion are closely related to another one, at first sight different: strains of the sliding and/or pinned state. It has long been known that the properties of sliding DWs are nonlocal[16] and are affected by contacts,[11] yielding thereby effects of phase slips, current conversion, etc. Recent years have brought a new understanding of the fact that the sliding state of DWs is also essentially inhomogeneous. A freedom for deformation is demonstrated by the dilemma associated with the choice of a solution for the generic equations describing the sliding motion and deformation of the CDW phase:

$$-\gamma\partial_t\varphi + K\partial_x^2\varphi = E, \quad E,\gamma,K = \text{const.} \tag{1}$$

Taken alone, Eq. (1) is satisfied by any solution of the type

$$\varphi = E\left(-\frac{c}{\gamma}t + \frac{(1-c)}{2K}x^2\right) \tag{2}$$

with an arbitrary value of the coefficient c. Then at first sight the response to the driving force E is optionally distributed between the viscous $\sim t$ and the elastic $\sim x^2$ reaction, leaving the collective current undetermined. We will see that it is specifically equilibrium with respect to phase slips that selects the solution $c=1$ and then leaves only the viscous nondeformed regime $\varphi \sim t$ in the bulk.

Local CDW deformations under the influence of an electric field have been studied by several *indirect* methods,[17] such as measurements of the shift of the local chemical potential along the sample using a laser probe,[18] electromodulated IR transmission,[19] and conductivity measurements on multicontacted samples.[16,20–22] On the other hand, x-ray measurements yield *direct* information on the spatial distribution of the CDW deformations. So far, a single experiment has been reported on $NbSe_3$:[24] the CDW deformation was monitored using a 0.8-mm-wide x-ray beam on a 4.5-mm-long sample. The data in Ref. 24 suggest an approximately linear variation of the satellite shift $q(x)=Q(x)-Q_0$ with x, in the central part of the sample, but experimental limitations did not allow the contact regions to be investigated. The recent precise space resolved determination of the shift $q(x)$ in Ref. 23 confirms that the CDW is deformed in the current carrying state with different effects near contacts and in the bulk. These experiments have given access to distributions and rates of phase slips and/or proliferation of edge dislocations across a sliding CDW. Similar effects of plastic flows are expected also in other types of electronic crystals and in vortex lattices. An original interpretation of the observed distortions ($q\neq 0$) came from the argument[25,24] that the energy $\sim U^* q$ of the density wave (DW) strain $\sim q$ at some effective stress U^* is opposed by the elastic energy $\sim Kq^2$ resulting in $q\sim -U^*/K$. It corresponds to the solution (2) with both terms being present, $c\neq 1$. The normal electrons as well as plastic processes (phase slips, dislocations) affect the stress $U^*(x)$ in such a way that it, and consequently q as well, increases near the injecting contacts giving rise to the ''phase slip voltage'' $V_{\rm ps}$.[11] This additional voltage has been interpreted[25] as a minimal stress required to create a supercritical D loop that can further expand across the sample providing a DW propulsion. Moreover it was argued that far from the contacts $U^*(x)\sim x$ following either (an earlier opinion[24]) the mean external voltage $U^*\Rightarrow\overline{\Phi}(x)=-\overline{\mathcal{E}}x$ or (a later point of view[21]) the phase slip stress $U^*\Rightarrow V_{\rm ps}(x/L)$ distributed over the length L between the contacts. While the predicted size dependence is different, in both cases one gets a constant wave number gradient $\partial q/\partial x = q'_{\rm blk}\neq 0$ in the bulk that is a parabolic phase profile $\varphi_{\rm blk}=q'_{\rm blk}(x^2/2)$ along the sample. This later point of view was claimed to bring agreement between theory and experiments, with quantitative discrepancies being largely eliminated (see[21] for a comprehensive review and Ref. 22) with changing to the second version: $U^*=V_{\rm ps}(x/L)$.

Our conclusions are opposite to those, derived from both the new high-resolution x-ray experiments,[23] qualitative theoretical statements[26] and from remodeling of both the present and earlier experimental data. We will show that for a long enough sample there must be *no linear gradient* like $q=q'_{\rm blk}x$ due to an applied or contact voltage. Instead we predict a strong dependence of $q'(x)$ near contacts that flattens (exponentially in the simplest case) towards the sample center. Our modeling shows that the large gradients earlier observed over the entire bulk in multicontact studies[21] are due to an *extreme size effect*: the distance between contacts was so short that only a small part ($\approx$16% according to our estimations) of the excess normal current is converted to the collective one and the partial currents are far from their mutual equilibrium values. Correspondingly the contact increment was small. On the contrary, the earlier x-ray experiments[24] have been performed on longer samples (as in the presently reported experiment), but could not resolve the contact region. What has been observed as a bulk gradient is consistent with our residual quenched distortion: it does not change between dc and pulsed experiments.

In the more recent x-ray experiments[23] the contact region has been resolved and deformations have been observed to

be large in comparison to the residual bulk gradient q'_{blk}. Evidence is found in favor of an *alternative effect*, namely the pinning or at least a strongly reduced climb of the *D*-lines, in some analogy to the pinning of individual vortices in superconductors, see review.[27] In the pulsed current experiments the observed decay of q near the contacts during the pulse delay, measured from 10^{-3}s to 10 s, resembles the Kim-Anderson law ($-\ln t$) for the supercurrent decay in superconductors via the creep of pinned vortices. Here we refer to the decay of the DW deformations near the contacts due to the backward creep of DLs during the long silent period between active pulses. The residual gradients in the bulk indicate that the current conversion is not complete ($\approx$90% is converted) so that the normal and collective currents have not reached their stationary equilibrium ratio.

II. EXPERIMENT

The measurements have been carried out on the diffractometers TROIKA I (ID 10A) and ID20 at ESRF (Grenoble, France) using an incident wavelength of 1.127 Å ($E=11$ keV) or 1.033 Å ($E=12$ keV), provided by a single Si(111) monochromator. High spatial resolution was obtained by reducing the beam width to 30 μm in the vicinity of the contacts (down to 10 μm at $T=110$ K).

The required *Q*-space resolution was obtained by using detector slits of 100 μm width, yielding a longitudinal resolution $\delta Q=6.8\times10^{-4}$ Å^{-1} at the (020) Bragg reflection of the sample. The mosaicity of the sample was found to be about 0.015°. The sample was oriented with the ($\mathbf{a}^*+\mathbf{c}^*,\mathbf{b}^*$) plane as the horizontal scattering plane. The major part of the measurements were carried out at $T=90$ K, in the upper CDW state ($T_{P_1}=145$ K; $Q_0=0.241b^*$) corresponding to the Peierls condensation of type-III chains.[28] A sample of cross section 10×2 μm^2 was mounted on a 100-μm-thick sapphire substrate, providing homogeneous sample cooling as well as adequate beam transmission ($\sim$50%). Electrical contacts were prepared by evaporating wide, 2-μm-thick gold layers onto the sample, leaving a free sample length of 4.1 mm between electrodes. The use of a substrate and the comparably low threshold current value ($I_T=2.16$ mA at $T=90$ K) allowed measurements to be performed not only with pulsed currents (pc) (100 Hz, 1% duty cycle) but also with direct currents (dc) up to 8 mA ($=3.7I_T$) without signs of Ohmic heating.

To erase any remnant deformation due to sample history, we applied a procedure analogous to that used in demagnetization or depolarization techniques, i.e., application of currents of alternating polarities and decreasing amplitude. We verified that this technique succeeds in recovering the original *zero-field* satellite position as well as the corresponding profile widths, along $\mathbf{b}^*$ and perpendicular to the chain direction (rocking width).

Figure 1 shows the $(0,1+Q_0,0)$ satellite profiles at $T=90$ K in reciprocal space along the $\mathbf{b}^*$ direction at the contact boundary (spatial position: $x=0$) measured with different direct currents. The position of the contact boundary is determined with an accuracy of ~10 μm from the excess ($\sim$10%) absorption of the deposited gold layer when sweeping the X-ray beam. When applying a 2-mA current, still

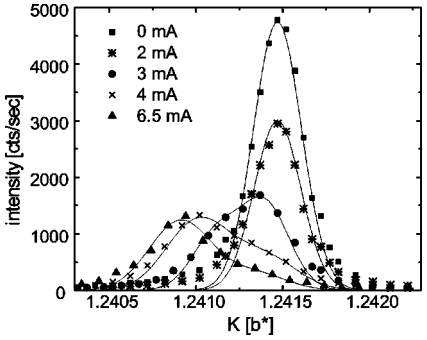

FIG. 1. Longitudinal satellite profiles at the contact boundary ($x=0$) for several applied direct currents; $NbSe_3$, $T=90$ K.

below the threshold current ($I_T=2.16$ mA), the satellite is not shifted with respect to its zero-current position but the peak intensity is already significantly reduced. This loss of peak intensity is recovered in the transversal broadening of the satellite profile. At higher currents, above I_T, the peak intensity is further reduced and the satellite position is shifted to lower values (with $I>0$) until a saturation is reached at high currents $I>2I_T$ both in peak intensity and satellite shift.[29] While the satellite profiles at zero current can be fitted with a single Gaussian, two Gaussians are needed in the sliding state. This peak splitting can originate either from a part of the x-ray beam hitting the electrode under which the CDW is always pinned and/or from the inhomogeneous current distribution in the close vicinity of the electrodes due to lateral current injection. However since we recorded similar splitting at several specific positions far removed from the electrode positions, we believe that the splittings reflect the inhomogeneous CDW motion, due to the presence of defects in the crystal bulk or due to steps at the surface. We find, additionally that the application of a dc current produces a larger shift ($\sim\times1.7$) than a pulsed current (100 Hz, 1% duty cycle) of same intensity.

The satellite shift at the contact boundary, as a function of applied direct current normalized to the threshold value, is drawn in Fig. 2 for temperatures $T=90$ K and 120 K. At 90 K, the satellite shift sets in at $I=I_T=2.16$ mA, increases strongly with $I>I_T$ and saturates for currents $I>2I_T$ at a satellite shift of $5.6\times10^{-4}b^*$. At 120 K, the threshold current is 0.8 mA. The current dependence follows a similar variation but with a much lower saturation of the satellite shift, namely $6\times10^{-5}b^*$.

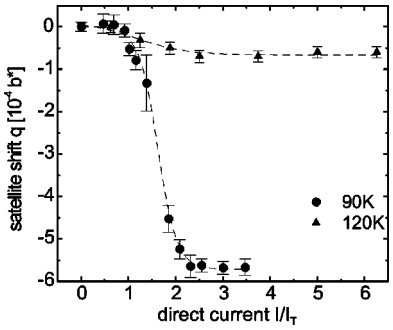

FIG. 2. Change of satellite position q for direct currents of varying intensities normalized to the threshold value I_t at the contact boundary; dots, $T=90$ K; triangles, $T=120$ K, $NbSe_3$; dashed lines are guides for the eye.

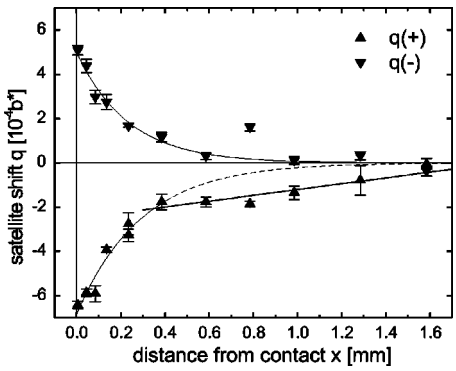

FIG. 3. q shift (in units of b^*) for positive (q_+) (negative q_-) applied direct currents ($I/I_T=3.52$), for one-half of the sample $0<x<2$ mm. The contact boundary is at $x=0$ (vertical grey line). The horizontal grey line is the line of zero shift. q_- is fitted with an exponentially decaying spatial profile, q_+ is fitted with an exponential decay near the contact boundary ($x<0.4$) and with a linear dependence in the central part of the sample. $NbSe_3$, $T=90$ K.

Figure 3 shows both shifts $q_+=Q(+I)-Q(0)$ and $q_-=Q(-I)-Q(0)$ as a function of beam position x along half of the sample ($0<x<2$ mm) for applied current $|I|=7.5$mA $=3.52I_T$ at $T=90$ K. For both polarities, the q shift reaches its maximum at the contact boundary, but with an asymmetry.

Such an asymmetry, already noticed in measurements of the spatial distribution of the CDW current with a multicontact setup,[22] is not yet clearly understood but seems to indicate that the current conversion mechanism at the electrodes is sensitive to the polarity of the driving electric field. For the negative polarity, $q_-(x)$ decreases continuously to zero in the central part of the sample with a law approximated by an exponential decay $\exp(-x/\lambda)$ with $\lambda=230\pm40$ μm. For the positive polarity, $q_+(x)$ shows a linear variation as a function of x in the middle of the sample with a slope of $(1.31\pm0.19)10^{-4}b^*mm^{-1}$; but close to the contact $0<x<0.4$ mm, $q_+(x)$ decays exponentially according to $\exp(-x/\lambda)$ with $\lambda=290\pm37$ μm.

In Fig. 4 we have drawn the ''double shift'' $q_\pm=Q(+I)-Q(-I)$ as a function of x for the same half of the sample for applied (pc and dc) currents of $|I|=4.6$ mA $=2.13I_T$. For dc currents, the spatial variation of $q_\pm(x)$ can be fitted with an exponential decay near the electrodes ($0<x<0.7$ mm) with a characteristic length of 375 ± 50 μm and a linear variation for 0.7 mm$<x<2$ mm with a slope of $\partial q_\pm/\partial x=-(2.0\pm0.1)10^{-4}b^*$ mm^{-1}[23]. It should be noted in Fig. 4 that in the middle part of the sample there is no observed difference between direct and pulsed currents. On the contrary the pc shift is nearly zero at the electrode position and reaches a maximum at a distance of about 100 μm away from the contact boundary. These differences suggest a spatially dependent relaxational behavior for the CDW deformations, the fastest relaxation occurring at the contact position. Keeping the pulse duration equal to 100 μs, we have measured the q shift for the positive polarity at $T=90$ K for a current $I=4.6$ mA as a function of the pause τ between pulses.

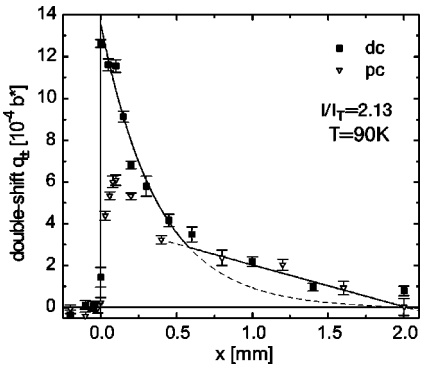

FIG. 4. Double-shift $q_\pm(x)=Q(I)-Q(-I)$ (in units of b^*) for direct (full squares) and pulsed (open triangles) current ($I/I_T=2.13$). The full line shows the exponential decay near the contact ($0<x<0.5$) and a linear dependence for $0.7<x<2$. The dash-dotted line extrapolates the exponential fit into the central section; $NbSe_3$, $T=90$ K.

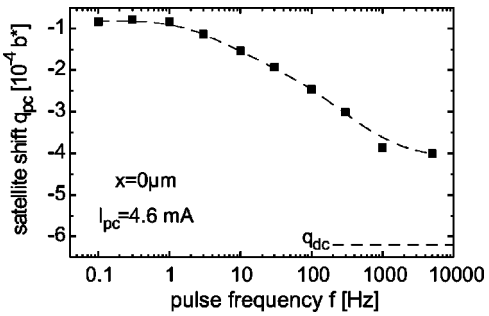

FIG. 5. Satellite shift q (in units of b^*) at the contact boundary as a function of the frequency $f=1/\tau$, τ: the time between current pulses ($I/I_T=2.13$). The dashed line represents the q shift for dc current of the same intensity; $T=90$ K.

Figure 5 shows the variation of q with frequency $f=1/\tau$. For the highest frequency (5 kHz) the shift reaches 70–80 % of the (maximal) dc shift. At low frequencies (0.1 Hz) q still has a finite value ($\sim$20% of the maximal dc shift) that reveals frozen deformations in the CDW condensate. The $q\equiv0$ value can only be attained by using the depolarization technique described above.

III. PARAMETERS AND MODEL-INDEPENDENT RELATIONS

Basic parameters relevant to $NbSe_3$ are the following: N_F/S is the density of states (DOS) above T_p where $S=a_\perp^2$ is an area per conducting chain and $N_F\approx0.3$ $(\mathrm{eV}A)^{-1}$, the normal conductivity at 90 K is $\sigma_n\approx3\times10^3$ $(\Omega\,\mathrm{cm})^{-1}$. In the upper CDW state there are two types $\alpha=i,e$ of normal carriers contributing to the total normal density $n_n=n_i+n_e$, current $j_n=j_i+j_e$ (both per chain and per electron) and the DOS $N_F=N_F^i+N_F^e$.

The intrinsic carriers, $\alpha=i$, originate from the condensed bands with metallic state Fermi level density of states N_F^i. Below T_p they are excited across the Peierls gap. In $NbSe_3$ between the two transitions the DOS part $N_F^i=\beta_iN_F$ for intrinsic carriers is closed by the DW gap and their energies are displaced when the Fermi level breathes changing $q(x,t)$ (see Ref. 30 for details). The extrinsic carriers $\alpha=e$ arise from uncondensed bands and their DOS part $N_F^e=\beta_eN_F$ is not closed by the DW. For $NbSe_3$, the two types of carriers

are associated to type-I and -II chains[28]. Microscopically their fractions β_i, β_e are expected to be close to 0.5.

It is of principal importance to distinguish between the potentials V_e, V_i, and V_c experienced by the extrinsic, intrinsic, and condensed electrons, respectively. In the condensed state the potential V_e experienced by extrinsic carriers is still the pure electric one: $V_e=\Phi$. But the potential $V_i=V$ experienced by intrinsic carriers is composed of Φ and of the potential due to the DW breathing $\sim q$:[30]

$$V_e=\Phi, \quad V_i=V=\Phi+q/\pi N_F^i. \tag{3}$$

The normal currents are driven by the effective electric fields E_α, which are gradients of their total chemical potentials μ_α,

$$E_\alpha=j_\alpha/\sigma_\alpha=-\partial\mu_\alpha/\partial x, \quad \mu_\alpha=V_\alpha+\zeta_\alpha(n_\alpha), \quad \alpha=i,e. \tag{4}$$

The local chemical potentials ζ_α can always be linearized in deviations δn_α (except for very low T in semiconducting DWs) and we have

$$\mu_\alpha=V_\alpha+\frac{\delta n_\alpha}{N^\alpha}, \quad N^\alpha=\frac{\partial n_\alpha}{\partial\zeta_\alpha}=\rho_\alpha N_F^\alpha, \quad 0<\rho_\alpha\leqslant 1. \tag{5}$$

The relative normal density ρ_i and the ''condensate'' density $\rho_s=1-\rho_i$ changes from $\rho_i=1,\rho_s=0$ in the metal state to $\rho_i=0,\rho_s=1$ at low T. At the same time $\rho_e\approx 1$ remains nearly constant. (The second DW transition at $T=59$ K closes N_F^e in $NbSe_3$. Then ρ_e becomes ''intrinsic'' with respect to the second CDW.) Fast equilibration of quasiparticles always leads locally to $\mu_i=\mu_e\equiv\mu_n$. The inhomogeneous electrochemical potential μ_n determines the normal current

$$j_n=-\sigma_n\frac{\partial\mu_n}{\partial x}, \quad \sigma_n=\sigma_i+\sigma_e, \tag{6}$$

where σ_n is the normal conductivity.[31]

A. Elastic and plastic deformations. Local relations

We separate the total charge density $n_{\rm tot}$ and the current density $j_{\rm tot}$ into their normal and condensate counterparts:

$$\delta n_{\rm tot}=\delta n_n+\delta n_c, \quad j_{\rm tot}=j_n+j_c \tag{7}$$

with

$$\delta n_n=\delta n_e+\delta n_i, \quad \delta n_c=\varphi_x/\pi, \quad j_c=-\varphi_t/\pi. \tag{8}$$

Here $\varphi_x=\partial\varphi/\partial x=q$ and $\varphi_t=\partial\varphi/\partial t$ stand for the local space and time derivatives of the CDW phase φ. The phase relations in the presence of dislocations are derived elsewhere.[26]

Finally, the potential of condensed electrons V_c coincides with the appropriately normalized CDW stress U. More specifically we define $2U$ as the energy per chain paid to distort the CDW elastically by one period 2π. Thus, U, as well as the strain q/π, refer to one electron in the ground state and it plays the role of a potential energy for the condensate electrons V_c. With this choice, U and the CDW driving force $\mathcal{F}=-\partial U/\partial x$ are additive to Φ and $E=-\partial\Phi/\partial x$, respectively. Being given by a variation of the local energy over q/π, the potential U includes contributions from three sources: the elastic stress, the stress provided by the excess concentration of intrinsic carriers, and the electric potential:

$$V_c\equiv U=(q/\pi+\delta n_i)/N_F^i+\Phi, \quad F=-\partial U/\partial x. \tag{9}$$

There are three main principal ingredients.

(a) The force F is equilibrated by the host lattice reaction, which is either the rest pinning force $F_{\rm pin}$ for $E<E_T$ or the friction force $F_{\rm frc}(j_c)$ for $E>E_t$. The equation $F=-F_{\rm frc}(j_c)$ or its inverse $j_c=J_c(F)$ are obtained from the bulk $V-I$ or $I-V$ characteristics of the sliding CDW.

(b) The exchange between the normal carriers and the condensate results finally in the equilibration between μ_n and U. Actually this process goes via proliferation of D lines or growth of D loops. This latter is controlled by the difference between $2\mu_n$ and $\mu_d=\partial W_d(N)/\partial N=\zeta_d+2U$, where N is the number of chains encircled by the D loop with a total free energy W_d, the internal chemical potential ζ_d arising from the entropy of defects or from the shape of the D loops.

(c) The local electroneutrality condition[32] implies that the variation of the carrier concentration n_n images the CDW wave number variations:[18]

$$\delta n_n=-\delta n_c=-q/\pi. \tag{10}$$

With Eqs. (3), (9), and (10) we can express q, at any x and t, as

$$gq/\pi N_F^i=\mu_n-U\equiv\eta, \quad g^{-1}=\left(\frac{\rho_i}{\rho_c}+\beta_e\right). \tag{11}$$

Here ρ_i and β_e characterize the screening of the CDW deformations by intrinsic and extrinsic carriers. As a whole, g is the normalized elastic constant since the total static energy density of the strained state is $(K/2)(\varphi_x/\pi)^2$ with $K=g/N_F^i$. At $T\to T_c$, $g\sim\rho_c\to 0$; at $T\ll\Delta$, $g\approx\beta_e^{-1}$, or for semiconducting DWs, $g\sim\rho_i^{-1}\sim\exp(\Delta/T)\to\infty$, which is the Coulomb hardening effect. In earlier studies U was supposed to be the elastic stress $\sim\rho_s q$, which appears opposing the electric field. Actually this conjecture, captured from the physics of neutral superfluid liquids is not quite applicable to the DWs. It has been shown[33] that the full stress $2U$, which includes Φ also, enters as the D-loop energy.

We see that the CDW is deformed whenever the stress U, the energy of condensed electrons, does not coincide with the electrochemical potential of the normal carriers μ_n. The quantity η characterizes this mismatch, and hence the excess or lack of normal carriers, which is measured directly by q. The exchange between the normal carriers and the condensate results finally in the equilibration between μ_n and $V_c\equiv U$, a process taking place via nucleation and growth of DLs. Differentiating Eq. (11) we arrive at

$$\frac{q'g}{\pi N_F^i}=F(j_c)-\frac{j_{\rm tot}-j_c}{\sigma_n}. \tag{12}$$

Since $g=g(T)$ is reasonably well known microscopically and $F(j_c)$ is known from the $V-I$ curves for nonperturbative distant contacts, then all observable quantities can be expressed locally and instantly via q, which is determined by the space resolved x-ray studies. Thus the DW current j_c is a solution of Eq. (12). This equation can be reduced to the one

used by the authors of Refs. 21 and 22, if we suggest that $F(j_c)$ may be decomposed to a major linear part plus pinning corrections and also ignore the structure of g in Eq. (11).

The equilibrium bulk current j_c is given by the above equation with the left-hand side (LHS) LHS=0. Then the electric field (relative to the extrapolated normal one at the same total current $j_{\rm tot}$) is

$$\Delta E = E - \frac{j_{\rm tot}}{\sigma_n} = -\beta_e \frac{j_c}{\sigma_n} - \beta_i \left(\frac{j_{\rm tot}}{\sigma_n} - F(j_c) \right). \tag{13}$$

This expression gives the nonlinear voltage: the increment with respect to the value extrapolated from below the sliding threshold. Other equivalent expressions for E may be useful in various circumstances:

$$E = \beta_e \frac{j_{\rm tot} - j_c}{\sigma_n} + \beta_i F(j_c) \quad \text{or} \quad E = \beta_i \frac{g q'}{\pi N_F^i} + \frac{j_{\rm tot} - j_c}{\sigma_n} \tag{14}$$

$$\text{or} \quad E = F(j_c) - \beta_e \frac{g q'}{\pi N_F^i}. \tag{15}$$

Here the first form provides a direct relation of E to j_c and hence to q' via (12). The second form involves the normal currents that can be measured independently. The third form requires attention: notice that the identification $E=F$, as usually assumed in the interpretation of experimental determination of the $I-V$ curves, is correct only in semiconducting DWs with $\beta_e=0$. In cases like $NbSe_3$ or semimetallic SDWs, only the simultaneous measurements of the two parameters (E and q' or E and j_n) allow one to extract the intrinsic characteristics $F(j_c)$, including the pinning threshold F_c, which are the fundamental properties we are looking for. The second form in (14) brings an important reassignment. We see that the measurement of E at known σ_n does not provide direct access to j_c which was a typical assumption in the analyses given in Refs. 21 and 22. Then the first equation in (14) shows that the discrepancy is maximal near the contacts [where $F(j_c)=0$]: we see the reduction by a β_c factor that is 50% for $NbSe_3$; thus, j_n is underestimated by a factor of 2. This effect comes from the fact that the extrinsic carriers move under the DW stress as well as under the electric field. The results of multicontact experiments need to be reconsidered in this view. The usual interpretation of the phase slip voltage also should be refined. Using the second form for E we obtain

$$V_{\rm ps} = \int_{\rm cnt}^{\infty} [E(x) - E(\infty)] = \frac{K}{\pi} q + \int_{\rm cnt}^{\infty} \frac{j_n(x) - j(\infty)}{\sigma_n} dx. \tag{16}$$

Here the first term coincides with the expected elastic stress at the contact. But we notice also an effective voltage from the excess of normal carriers that gives a comparable contribution. Finally notice that experimentally one usually extracts the current increment for which there are no convenient expressions. In general, monitoring the current gives a simpler access to internal processes than a more usual monitoring of the voltage.

B. Mechanisms for the current conversion

The local relations (11) must be supplied with boundary conditions and with a law for the current conversion due to DL nucleation. (For brevity we do not consider the transient DW current in multicontact configurations). The boundary condition at the outermost contacts $x_{\rm cnt}$ is straightforward: $j_n(x_{\rm cnt}) = j_{\rm tot}$, $j_c = 0$. The asymptotic condition far from the contact is more subtle and it turns out to be one of the points that distinguishes our picture from other recent treatments, e.g., Ref. 25. Namely, the condition that all partial currents are stationary in the sample bulk implies the absence of current conversion, all types of carriers being in equilibrium, with equal chemical potentials $\mu_n = \mu_d/2$. Furthermore, allowing for large D loops or nearly straight D lines reduces μ_d down to $2U$. Then we see from (11) that $q \to 0$, which proves our statement on the absence of deformations in the free sliding regime.

The balance between the different types of carriers is controlled by the injection/extraction rates from the electrodes and by the conversion rate R between normal carriers and condensed carriers. The conversion rate can always be decomposed into passive and active contributions as

$$R(\eta, j_c) = R_p(\eta) + R_a(\eta, j_c).$$

There are two extreme scenarios for the passive conversion. The first refers to an ideal host crystal, both in the bulk and at the surface, where only *homogeneous* nucleation is present as a spontaneous thermal[25] or even quantum[34] supercritical fluctuation, so that

$$R = R_0 \exp[-\eta_0/|\eta|], \quad \text{or at } T \to 0,$$

$$R = R_0 \exp[-(\eta_0/\eta)^2]. \tag{17}$$

This frequently exploited form is valid asymptotically at $\eta \to 0$. Actually the so-called attempt rate $R_0 \neq \text{const}$, $R_0 \sim \eta^\alpha$ with the index α dependent on dimension and on microscopic mechanisms of aggregation of electrons to the DL. So for η being not too small, the power laws will dominate over the exponential one.

A quantitative analysis of the passive DL nucleation requires a determination of the characteristic time scale τ_0. Usually $1/\tau_0$ is identified with an attempt rate derived from microscopical parameters like a phonon frequency. It seems that in CDWs the rate is rather limited by the ability of electrons to concentrate in required volume (of a size of D loop) for a sufficient time. Hence $\tau_0 = \mathcal{R}C$, where $\mathcal{R}$ and C are the resistance and the capacitance of the corresponding volume. Conveniently in a three-dimensional (3D) geometry this product does not depend on the length scale $\tau_0 = f(r_\parallel/r_\perp)/\tilde{\sigma}$, where $\tilde{\sigma}$ is a relevant conductivity, most probably the normal perpendicular one $\tilde{\sigma} \sim \sigma_n^\perp$, and $r_\parallel, r_\perp$ are characteristic sizes of the nucleation region.

Another *heterogeneous* extreme refers to samples with a sufficiently large density of imperfections acting as nucleation centers for supercritical DLs, the simplest form for this case being $R \propto \eta$. Since $\delta\eta = -q\,\delta n_n g/N_F^i$, then the law $R = \Gamma_p N_F^i \eta$ is equivalent to $\delta\dot{n} = -\delta n/\tau_{\rm cnv}$. Indeed

$$-\delta\dot{n}_n = \delta\dot{n}_c = 2g\Gamma_p \delta n_n = \delta n_n/\tau_{\rm cnv}, \quad \tau_{\rm cnv} = (2g\Gamma_p)^{-1}.$$

Here $\tau_{\rm cnv}$ is the lifetime of an excess carrier with respect to its conversion to the condensate, that is the mean free time before an absorption by a DL. Both of the above scenarios are of the ''*passive*'' type, when the DW motion itself plays no role. A plausible ''*active*'' scenario emerges for a fast enough DW motion when the DLs are created by the DW sliding through bulk or surface defects $R=R(\eta,j_c)$, such that $R(0,j_c)=R(\eta,0)=0$ with $R\propto\eta j_c$ as the simplest version. The condition $R(0,j_c)=0$ tells us that the creation of a DL by the current is not sufficient. An active process in the bulk corresponds to the creation of pairs of dislocation loops[35–37] at strong impurities, thus providing for a local slowing down of the DW motion. If also $\eta\neq 0$ then loops of one sign will have a higher probability to survive and finally to aggregate into larger ones. Another branch of this scenario, possibly the most realistic one for clean thin samples, relies upon the ultimate creation of *D* lines at crystallographic steps on the surface. The current being forced to cease (for inward steps) or start (for outward steps), a whole *D* line must be created after each DW period. The active mechanism may dominate at large enough j_c but it cannot trigger itself from zero. There must be either a passive contribution or a finite $j_c\neq 0$ at the boundary. The last case implies that the conversion is exceptionally efficient at the very edge of the contact, which is quite plausible; in this case, a part of the normal current would be converted within a narrow layer beyond the experimental resolution.

Whatever the mechanism for the creation of *D* lines or *D* loops, their subsequent propagation across the sample is affected by interaction of these lines with impurities. As known from the theory of vortex lines and from the experience with supercurrent decay in superconductors, such a line is subjected to a collective or a local pinning, see Ref. 27. The collective pinning implies the existence of a critical value η_t below which the motion is hindered, the DL will not expand so that $R=0$ if $|\eta|<\eta_t$. We associate the small residual gradient $q'_{\rm blk}$ to this effect. An important observation is that its value does not change between dc and pulsed experiments. This tells us that the associated deformation is frozen in. Since in dc experiments the DW body pinning is overcome, it is natural to invoke a plastic pinning mechanism like the pinning of *D* lines.

A similar phenomenon, but in reverse order, seems to be observed in the contact region in pulsed experiments. Since the scattering intensity is accumulated mostly through the passive intervals between the pulses (typically several orders of magnitude longer than the active pulses), what one then observes is a residual quenched deformation. Presumably the same mechanism that causes the observed pinning of remnant *D* lines in the bulk here prevents the backward motion of excess *D* lines in the contact region. Actually at very long times, the thermal climb, similar to the creep of vortices, will allow for DW propagation and the contact deformation will eventually decay.

Present preliminary results on the dependence of q on pulse frequency are consistent with this scenario. Indeed, the decay time of q as measured at a fixed point near the contact, as shown in Fig. 2, has a clear logarithmic character. The analogy to the Kim-Anderson law in the case of superconductors is transparent: the propagation of *D* lines works to relax the strain $\partial\varphi/\partial x$ in the same way as the vortices of the superconducting phase χ work to relax the supercurrent $j_s\sim\partial\chi/\partial x$.

The boundary between the contact regions, where q changes with time and the middle part where it does not, tells us about the crossover from local DL pinning (leading to creep) to collective pinning below the threshold stress η_t.

IV. STATIONARY DISTRIBUTIONS FOR VARIOUS CONVERSION LAWS: THEORY VERSUS EXPERIMENT

The equation for the stationary distribution of the CDW deformation can be obtained directly from Eqs. (3), (9), (11) as

$$\frac{\partial\eta}{\partial x}=F(j_c)-\frac{(j_{\rm tot}-j_c)}{\sigma_n}, \tag{18}$$

which follows from the definition of η and the current partition $j_n=j_{\rm tot}-j_c$. Equation (18) should be combined with the relation:

$$\partial j_c/\partial x=2R(\eta,j_c),$$

which results from the carrier conservation law

$$\partial(\delta n_c)/\partial t+\partial j_c/\partial x=d(\delta n_c)/dt=2R$$

with $\partial(\delta n_c)/\partial t=0$ in the stationary case.

The function $F(j_c)$ or its reciprocal $j_c=j_c(F)$ can be taken from the experiments on long samples, e.g., it can be modeled by the standard Bardeen parametrization[38] valid empirically except in the close vicinity of F_t:

$$J_c(F)=\sigma_\infty(F-F_t)\exp\left[-\frac{kF_t}{F}\right],\quad k\approx 1.1. \tag{19}$$

Consider the simplest case of a heterogeneous, passive nucleation of DLs:

$$R=R_p(\eta)=\Gamma_p N_F^i\eta. \tag{20}$$

Suppose also that the driving force is linear, $F(j_c)=j_c/\sigma_c$. Then the solution of Eqs. (18) and (19) is

$$\eta=-\frac{j_{\rm tot}}{\sigma_n}\lambda\frac{\sinh x/\lambda}{\cosh a/\lambda} \tag{21}$$

(for contacts at $x=\pm a$). Here $j_{\rm tot}$ is the total current applied at the contacts and λ is the characteristic length scale of the phase slip distribution. Equation (21) shows explicitly that for a long enough sample $a\geqslant\lambda$ there will be no linear gradient in the bulk. The carrier conversion will be nearly complete and the CDW deformation will reduce to zero. For short spacing $a\leqslant\lambda$ we find a linear variation $\eta\approx -xj_{\rm tot}/\sigma_n$ which is a consequence of a negligible current conversion. For λ we obtain

$$\lambda=r_D\sqrt{\frac{4\pi}{\beta_i}g\sigma^*\tau_{\rm cnv}},\quad r_D=\left(\frac{S}{4\pi e^2N_F}\right)^{1/2}\sim 1\text{Å}. \tag{22}$$

At a given current $q'\sim(\sigma_n g)^{-1}$; then near T_c, $g\sim(T_c-T)$, while $\sigma_n\approx$ const and we find that just at the contact the gradient of the deformation increases but may not be

visible because the length scale shrinks as $\sqrt{(T_c-T)}$. The q values grow as $q\sim 1/\sqrt{(T_c-T)}$. For semiconducting DWs at low T the fast, activational, T dependences of $\sigma^*\approx\sigma_n \sim\rho_n, g\sim\rho_n^{-1}$ cancel in expressions for q' and λ. Hence q' will be a smooth function while $\lambda(T)$ and $q(T)$ will grow as $\tau_{\rm cnv}^{1/2}$.

The electric field can be found as

$$E=\frac{j_{\rm tot}}{\sigma_n+\sigma_c}+\eta'\sigma^*\left(\frac{\beta_e}{\sigma_n}-\frac{\beta_i}{\sigma_c}\right),$$

which gives us the phase slip voltage

$$V_{\rm ps}=-\sigma^*\left(\frac{\beta_e}{\sigma_n}-\frac{\beta_i}{\sigma_c}\right)\eta|_{\rm cnt}.$$

Since at the contact $\eta\approx(j_{\rm tot}/\sigma_n)\min\{a,\lambda\}$, we obtain

$$\frac{V_{\rm ps}}{\overline{V}}=\left(\beta_i-\beta_e\frac{\sigma_c}{\sigma_n}\right)\min\{1,\lambda/a\},\quad \overline{V}=\frac{2aj_{\rm tot}}{\sigma_n+\sigma_c},$$

where $\overline{V}$ is the bulk voltage across the sample of length $2a$. Notice that $V_{\rm ps}\sim j_{\rm tot}$ rather than being an intrinsic activation energy. Notice also the opposite sign of the contribution from extrinsic carriers. The opposite polarization of i and e carriers has already been noticed in the linear electrodynamics of CDW.[30]

Applying Eq. (21) to our dc data, one obtains a very satisfactory fit of the spatial variation of $q_\pm(x)$ from the contact position $x=0$ to $x=0.5$ mm with the characteristic length scale of the phase slip distribution $\lambda=375\ \mu$m$\pm 50\ \mu$m (at $I_{\rm CDW}=2.1I_T$). However, the observed linear variation of q in the central part of the sample (Fig. 2) suggests that the conversion rate may be suppressed by pinning of the DLs below some finite nonequilibrium threshold η_t: $R=0$ if $|\eta|<\eta_t$. In this latter case, the carrier conversion is blocked and the normal and collective current densities, j_n and j_c, are fixed at values above (j_n) or below (j_c) their equilibrium values. We then see from Eq. (18) that $\partial\eta/\partial x=\eta'_{\rm blk}=$const$\neq 0$, thus $\eta(x)=\eta'_{\rm blk}x$ and therefore $q\propto x$, in agreement with the data in Fig. 2. More generally, numerical simulations of stationary solutions of Eq. (18) can be obtained for various types of conversion mechanisms and from the j_c dependence of $F(j_c)$ obtained from experimental I–V curves.[26]

Knowing the value of λ we can estimate the phase slip rate or the conversion lifetime,

$$\tau_{\rm cnv}=\left(\frac{\lambda}{r_D}\right)^2\frac{\beta_i}{4\pi g}\frac{1}{\sigma^*}\sim\left(\frac{3\times10^{-4}}{10^{-8}}\right)^2\frac{1}{25g}10^{-13}\sim\frac{4}{g}10^{-6}\ \text{s}.$$

Since $g\sim 1$ at $T\approx 90$ K, then the conversion rate is within the range of MHz. This crossover frequency separates the two regimes of the CDW electrodynamics: a quasiequilibrium one at low frequencies and the two-fluid one in the high frequency. To our knowledge, this division has never been taken into account in earlier theoretical studies and in interpretations of microwave experiments. The time-dependent equations will be described elsewhere.[26]

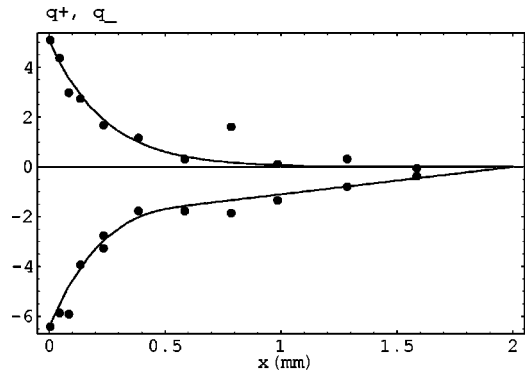

FIG. 6. Calculated $q(x)$ profile for positive (q_+) (negative q_-) applied direct currents ($I/I_T=3.52$) against experimental data shown in Fig. 3.

V. MODELING UNDER EXPERIMENTAL CONDITIONS

Below we shall give several examples of simulations under real experimental conditions relevant to our experiments: distances between contacts are $L=2a=4$ mm, the total currents are $j_{\rm tot}=3.5I_T$ and $2.13I_T$. We have tried the following forms for R, see discussion in Sec. III B.

(I) Heterogeneous nucleation (passive plus active contributions),

$$R=R_p\eta+R_a\eta j_c. \tag{23}$$

(II) Homogeneous nucleation,

$$R=R_0\exp[-\eta_0/|\eta|]. \tag{24}$$

In all cases we also try a quenched version with $R=0$ at $|\eta|<\eta_t$, where the potential η_t is a threshold below which the pinning of D lines is stronger than the oversaturation.

Figure 6 presents our simulation for the shift q at the current $I=3.5I_T$. The q shift (in units of b^*) for positive (q_+) (negative q_-), for one-half of the sample $0<x<2$ mm plotted against experimental data from Fig. 3. The contact boundary is at $x=0$.

Taking from the experimental data the contact value of $q_{(+)\rm cnt}\approx 6.425\times10^{-4}b^*$ for positive, $q_{(-)\rm cnt}\approx 5.09\times10^{-4}b^*$ for negative current polarity and assuming $g=1$, $b^*=1.8$ Å^{-1}, we determine the contact overstress $\eta_{(+)\rm cnt}\approx 1.2$ meV and $\eta_{(-)\rm cnt}\approx 0.97$ meV. From our fit the cutoff value $\eta_t\approx 0.32$ meV is in a good agreement with the value $\eta_t\approx 0.35$ meV estimated from the persistent gradient in the middle of the sample for positive current polarity. The ratio of passive to active conversion is $R_p/R_aI_{\rm CDW}\approx 2.1$, so the active conversion contributes to about 30% of the total.

Figure 7 gives the distribution of the CDW current $I_{\rm CDW}/I_T$, dashed line, and of the electric field $(E-E_{\rm blk})/F_T$, solid line, for $I=3.5I_T$. The parameters have been determined from our best fit of $q(x)$ in Fig. 3. The midpoint of the sample corresponds to $x=2$ mm.

Figure 8 shows the distribution $2q(x)$ for $I=2.13I_T$ plotted against the double-shift data of dc experiments, Fig. 4. The x axis gives the distance from the left contact at $x=-2$ mm to the midpoint of the sample $x=0$. The y axis gives $2q$ (double shift) in units of $10^{-4}b^*$. Taking from the data the contact value of $2q_{\rm cnt}=12.6\times10^{-4}b^*$ assuming g

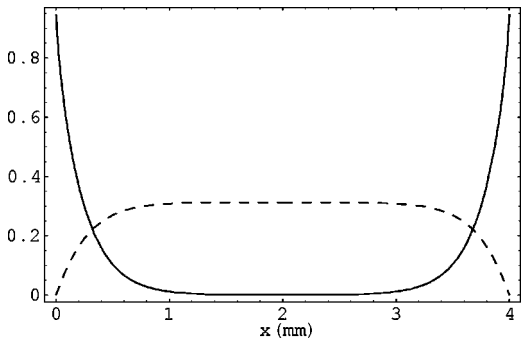

FIG. 7. Calculated distributions of the CDW current j_c/I_T (dashed line) and of the electric field $(E-E_{\rm blk})/F_t$ (solid line) between electrodes ($x=0$, $x=4$ mm) for the best fit of the $q(x)$ profile in Fig. 3 ($I/I_T=3.52$).

$=1$, we determine the contact overstress $\eta_{\rm cnt}=1.2$ meV. From our fit we have the cutoff value $\eta_t=0.24$ meV in a good agreement with the estimate based on the persistent gradient in the middle $q_{\rm blk}=1.10^{-4}$ Å^{-1}, which gives $\eta_t=0.25$ meV. A comparison of the passive and active conversion mechanisms is given by the ratio $R_p/R_aI_{\rm CDW}\approx 1.2$ determined from our fit. In this case the two contributions are comparable. We have also done the simulation for the same parameters as for Fig. 8 but without the cutoff: $\eta_t=0$, dashed line on Fig. 8. While the contact region is fitted well, the middle part does not reproduce a finite gradient.

Notice that in both cases ($I=3.5I_T$ and $I=2.13I_T$) none of passive and active conversion mechanisms taken separately is able to provide a satisfactory fit of the experimental data for the regime with essentially nonlinear I-V (the model with the linear I-V is well fitted in both cases with linear $R_p\sim\eta$ alone).

We have also done the fit relevant to the multicontact experiments[21] using the same model as for the Grenoble experiment. Now the distance is short $L=670$ μm and the current is high $I=5I_T$. We obtained that there is *no visible difference* between the solutions with and without cutoff. Hence in experiments[21] the entire sample length is influenced by the contacts, the partial currents are far from equilibrium, and conversion takes place over the entire sample but is far from being complete.[26]

A comparison between the two sets of x-ray measurements[23,24] in the middle of the sample indicates that

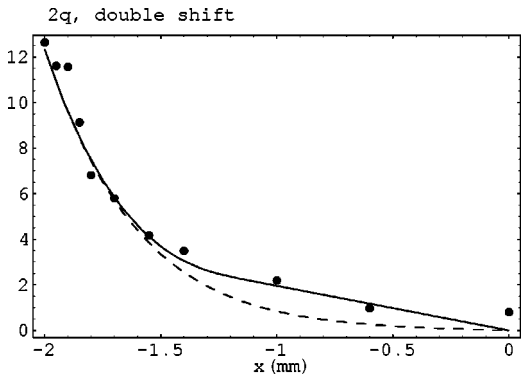

FIG. 8. Calculated $2q(x)$ profile ($I/I_T=2.13$) against experimental data shown in Fig. 4. The dashed line shows the same fit but without cutoff $\eta_t=0$.

the cutoff value η_t in the Cornell sample[24] is about twice higher than in the Grenoble one.[23] It is clear that the Cornell x-ray data show the effect of a quenched gradient of the same origin as in the Grenoble experiment, but not the phase slip stress transferred from the contacts as suggested by the authors. The x-ray and multicontact experiments refer to completely different regimes.

Our fitting allows an estimate of mean concentration (per unit sample cross section) of lattice faults $N_{\rm flt}$ contributing to the active conversion mechanism. We shall view those faults as line objects, perpendicular to the chain axes, most probably as crystal-shape steps. We have

$$2R_a(\eta,j_c)=\frac{dj_c}{dx}=PN_{\rm flt}j_c, \tag{25}$$

where P is the probability to create a supercritical D line at one fault per one DW period. Our hypothesis $R_a\sim\eta j_c$ means that $P(\eta)=\eta/\eta^*$ where the constant η^* is determined by the condition $P(\eta^*)=1$. Hence η^* can be estimated as the stress sufficient to unbound the tightest D line that is just at one layer from the surface. Since the normal to the surface direction in $NbSe_3$ corresponds to the weakest interchain (actually the interplane) coupling characteristic of semiconducting materials (of the order of T_p), we expect $\eta^*\sim 100$ K. Now

$$N_{\rm flt}=2\eta^*R_a\approx 10^{-5}\ \text{Å}^{-1}.$$

We have obtained the distance $L_{\rm flt}=1/N_{\rm flt}\sim 10$ μm, which is less but comparable to the initial decay scale $(q/q')_{\rm cnt}\sim 60$ μm and 30 times below the total characteristic length 300 μm. We see that the current conversion is provided by about 10^1-10^2 crystal defects with a maximal (near the contact) efficiency of a few percent, $\eta_{\rm cnt}/\eta^*\sim 0.1$. We conclude that D loops of opposite signs predominantly annihilate each other by exchanging locally the normal currents and only some fraction survives to proliferate across the sample.

VI. DISCUSSION

The conclusions we derive from our high-resolution x-ray measurements and from the above theory are as follows. For a long enough sample the large $q(x)$ values near the contacts decrease (exponentially in the simplest case) towards zero at the sample's center. The large gradients observed in earlier multicontact studies[21] can now be reinterpreted as due to an extreme size effect: the distance between contacts is so short that only a small part of the applied normal current is converted, so that the currents j_c and j_n stay far from their equilibrium values. In such a case, $q(x)$ is close to linear with only small contact increments. For longer samples (4.5 mm), as was used in x-ray experiments, these deformations leave the bulk free and concentrate near the contacts. Earlier x-ray experiments[24] could not resolve the contact region and what was observed as a bulk gradient coincides with our residual distortion $q'_{\rm blk}$ from pinned deformations.

The earlier x-ray experiments[24] have been performed using only pulsed currents when the intensity is collected predominantly through passive intervals with zero current. It was suggested that the gradients formed during the active pulses do not relax during the long passive intervals, thus

allowing for a finite q shift. This picture seems to be contradictory: if the relaxation is supposed to be long enough to preserve the state of the preceding active interval during the long passive one, then the active interval becomes much too short for establishing the steady-state configuration adequate to injection or applied voltage. Then, one may think that what was observed actually were the residual distortions quenched by some kind of pinning, at first sight by the conventional pinning[39] of the DW body. The Grenoble experiments, performed both in pulsed and dc regimes, undermine the possibility of body pinning by showing that the ''residual'' distortions are present invariably also in dc regime where the body pinning has been overcome. Hence there is a request for another type of pinning present for the DW both in motion and at rest. The picture we have for the origin of these gradients is the pinning of D lines, thus hindering the current conversion.

An important observation is that this gradient does not change between dc and pc experiments, indicating that the associated deformation is quenched. A related pinning phenomenon is observed in the *contact* region in *pulsed* experiments. Noting that 99% of the x-ray intensity is accumulated during the passive intervals between current pulses, we conclude that the observed pc shifts correspond to pinned deformations, which remain quenched on the time scale of the pulse interval. At very long times, thermal climb, similar to vortex creep, will allow for DL propagation and for the eventual decay of the deformation. Our preliminary results on the dependence of q on pulse frequency are in favor of this scenario.

Our definite choice for an heterogeneous DL nucleation scenario comes from the observation of the partially localized character of the deformations near the contact, whereas the homogeneous scenario would lead to an extremely slow $\sim 1/\ln(x-x_{\mathrm{cnt}})$ decay of the deformations. An intriguing question therefore arises: Why is a value of the decay length λ found in the present measurements so similar to that obtained from multicontact and optical measurements on semiconducting CDWs (Refs. 19 and 20), where a drastic T dependence of λ is expected due to the freezing of the normal carriers. A tentative answer can be derived from the linearized model (Sec. IV), which shows that the concentration of normal carriers affects the quantities g and σ^* in opposite senses ($g\sim 1/\rho_n$, $\sigma^*\sim\rho_n$) leaving $\lambda\sim(\sigma^* g)^{1/2}$ following Eq. (22) invariant. Finally $\lambda\sim\sqrt{D_n\tau_{\mathrm{cnv}}}$ appears to be clearly related to the one-electron diffusion length with respect to its absorption to the condensate, independent of the free carriers concentration. This important cancellation supports our model and the argument that the conversion rate dependence is primarily $\mathcal{R}\sim-\delta n$, while the law $\mathcal{R}\sim\eta$ appears as a consequence due to local relations $-\delta n=q/\pi$ and $q\sim\eta$.

VII. CONCLUSIONS

Till now the DW ability to slide and to be deformed were assumed to be closely related. Our results show that they rather exclude each other. In the sliding state the DW carries its fraction of the total current that can reach, far from contacts, a value corresponding to the parallel circuits of normal and collective conductances. This state is reached only when the DW is unbound from contacts and the equilibration between the normal current and the collective one is completed. In contradiction to earlier theoretical expectations and interpretations of experiments, we show that this state is mainly undeformed. Namely, elastic deformations, either from the distributed stress (as it has been conjectured originally[25,24]) or from the phase slip tension at the contacts (as it has been supposed later[21]), are incompatible with an equilibrium with respect to the conversion. Notice that the first multicontact experiments performed on semiconducting TaS_3 (Ref. 20) have already revealed a dominance of contact deformations and their shrinking with increasing current in accordance with our modeling.

Our results show that the contact deformations can spread over large distances from the contacts, as long as the partial currents are not equilibrated. The strong linear dependence of the DW wave number $q(x)$ inferred earlier from the multicontact experiments must be reinterpreted as ''ballistic,'' with respect to current conversion, a regime when most of the normal carriers pass along the sample length without initiating the necessary climb of dislocations. The DW current and the total conductivity are then expected to be smaller than their nominal values. Also, the enhancement of the deformations near the contacts should be relatively small as the simulations in Ref. 21 actually show. In contrast, the x-ray experiments in Grenoble are characterized by strong effects near contacts and by relatively weak but stable (e.g., persistent through the passive intervals in pulsed experiments) gradients through the middle part. This tells us that the conversion is hindered below some threshold value of the parameters describing the departure from equilibrium. In that case the DW current stays below its nominal value, but deformations are allowed at this expense. Hindering of the current conversion gives information on the pinning of the dislocation lines that persists even in the sliding state when the pinning of the DW body has been overcome. It is the same quenched regime in the bulk that has been observed in earlier x-ray studies,[24] since the contact regions were not accessible.

We believe our results illustrate a number of important common features to the physics of all different sliding superstructures. The elaborate picture presented here should be taken into account also in studies of 2D electronic crystals and of vortex lattices.

ACKNOWLEDGMENTS

The authors are indebted to M. Brunel (Cristallographie/CNRS) for making possible the x-ray characterization of the samples and to H. Berger and F. Levy (EPFL Lausanne) for providing the $NbSe_3$ samples. H. Requardt acknowledges financial support by an ''Allocation de Recherche'' from the French Ministry of Education and Research (MESR). F. Ya. Nad' was partly supported by the Russian Fund of Basic Research C Grant No. 99-02-017364.

*Present address: Max-Planck Institut f. Metallforschung, Heisenbergstrasse 1, D 70569 Stuttgart, Germany.
[1] P.W. Anderson, *Basic Notions of Condensed Matter Physics* (Benjamin Cummings, New York, 1984).
[2] J.S. Langer and V. Ambegoakar, Phys. Rev. **164**, 498 (1967).
[3] B.I. Ivlev and N.B. Kopnin, Adv. Phys. **33**, 47 (1984).
[4] E. Varoquaux and O. Avenel, Physica B **197**, 306 (1994).
[5] *Charge Density Waves in Solids*, edited by L.P. Gor'kov and G. Grüner, Modern Physics in Condensed Matter Science Vol. 25 (North-Holland, Amsterdam, 1989).
[6] S. Brazovskii and P. Monceau, J. Phys. IV **3**, C2 (1993).
[7] S. Brazovskii and P. Monceau, J. Phys. IV **9**, 10 (1999).
[8] G. Grüner, *Density Waves in Solids* (Addison-Wesley, Reading, MA, 1994).
[9] L.P. Gor'kov, Pis'ma Zh. Éksp. Teor. Fiz. **38**, 76 (1983) [JETP Lett. **38**, 87 (1983)]; and in *Charge Density Waves in Solids* (Ref. 5).
[10] N.P. Ong and K. Maki, Phys. Rev. B **32**, 6582 (1985).
[11] J.C. Gill, J. Phys. C **19**, 6589 (1986); J. Phys. IV **3**, 165 (1993).
[12] J. Dumas and D. Feinberg, Europhys. Lett. **2**, 555 (1986).
[13] D. Feinberg and J. Friedel, J. Phys. (France) **49**, 485 (1988).
[14] S. Brazovskii, Sov. Phys. JETP Lett. **28**, 606 (1978); Zh. Éksp. Teor. Fiz. **78**, 677 (1980) [JETP Lett. **51**, 342 (1980)].
[15] For a review see S. Brazovskii in, *Charge Density Waves* (Ref. 5), p. 425.
[16] M.C. Saint-Lager, P. Monceau, and M. Renard, Europhys. Lett. **9**, 585 (1989).
[17] For a review, see F.Ya. Nad, in *Charge Density Waves* (Ref. 5), p. 193.
[18] M.E. Itkis, F. Ya. Nad, and V.Ya. Pokrovskii, Zh. Éksp. Teor. Fiz. **90**, 307 (1986) [JETP **63**, 177 (1986)].
[19] M.E. Itkis, B.M. Emerling, and J.W. Brill, Phys. Rev. B **52**, R11 545 (1995).
[20] M.E. Itkis, F. Ya. Nad, P. Monceau, and M. Renard, J. Phys.: Condens. Matter **5**, 4631 (1993).
[21] T.L. Adelman, M.C. de Lind van Wijngaarden, S.V. Zaitsev-Zotov, D. DiCarlo, and R.E. Thorne, Phys. Rev. B **53**, 1833 (1996), and references therein.
[22] S.G. Lemay, M.C. de Lind van Wijngaarden, T.L. Adelman, and R.E. Thorne, Phys. Rev. B **57**, 12 781 (1998).
[23] H. Requardt, F.Ya. Nad, P. Monceau, R. Currat, J.E. Lorenzo, S. Brazovskii, N. Kirova, G. Grübel, and Ch. Vettier, Phys. Rev. Lett. **80**, 5631 (1998).
[24] D. DiCarlo, E. Sweetland, M. Sutton, J.D. Brock, and R.E. Thorne, Phys. Rev. Lett. **70**, 845 (1993).
[25] S. Ramakrishna, M.P. Maher, V. Ambegaokar, and U. Eckern, Phys. Rev. Lett. **68**, 2066 (1992).
[26] S. Brazovskii and N. Kirova, Synth. Met. **103**, 2589 (1999).
[27] G. Blatter *et al.*, Rev. Mod. Phys. **66**, 1125 (1994).
[28] E. Canadell *et al.*, Inorg. Chem. **29**, 1401 (1990).
[29] Hereafter we are using notations I for total currents across the sample and j for currents per chain and per electron.
[30] S. Brazovskii, J. Phys. I **3**, 2417 (1993); J. Phys. IV **3**, 267 (1993).
[31] Hereafter we imply that all σ's include an additional factor S/e^2 reflecting that all our quantities are defined per chain per electron.
[32] S. Artemenko and A. Volkov, in *Charge Density Waves in Solids* (Ref. 5), p. 365.
[33] S. Brazovskii and S. Matveenko, J. Phys. I **1**, 269 (1991); **1**, 1173 (1991).
[34] K. Maki, Phys. Lett. A **202**, 313 (1995).
[35] S. Brazovskii, in *Proceedings of the NATO Summer School, Les Houches '95*, edited by C. Schlenker and M. Greenblatt (World Scientific, Singapore, 1996).
[36] A. Larkin and S. Brazovskii, Solid State Commun. **95**, 275 (1995).
[37] S. Brazovskii and A. Larkin, Synth. Met. **86**, 2223 (1997).
[38] J. Bardeen, Phys. Rev. Lett. **42**, 1498 (1979); **45**, 1978 (1980); **55**, 1010 (1985); Physica B & C **143**, 14 (1986); Phys. Scr. **T27**, 136 (1989).
[39] P.A. Lee and T.M. Rice, Phys. Rev. B **19**, 3970 (1979).